Positive Allosteric Modulation of the α5-GABAA receptors prevents neuronal atrophy and cognitive decline independently of tau tangle accumulation in the PS19 mouse model

Ravinder N. Dharavath[1+], Ashley M. Bernardo[1+], Cassandra Marceau-Linhares[1+], Michael Marcotte[1], Kayla Wong[1], Celeste Pina-Leblanc[1], Adrien Bouchet[1], Dishary Sharmin[2], Kamal P. Pandey[2], James M. Cook[2], Thomas D. Prevot[1,3,4*], Etienne L. Sibille[1,3,4*]

[1]Campbell Family Mental Health Research Institute of CAMH, 250 college street, Toronto, ON, M5T 1R8 Canada

[2]Department of Chemistry and Biochemistry, University of Wisconsin–Milwaukee, 3210 N Cramer Street, 53211, WI, USA

[3]Department of Psychiatry, University of Toronto, 250 college street, Toronto, ON, M5T 1R8 Canada

[4]Department of Pharmacology and Toxicology, University of Toronto, Medical Sciences Building, 1 King's College Cir Room 4207, Toronto, ON, M5S 1A8, Canada

[+]These authors equally contributed to the study

[*]Corresponding Authors:

Etienne Sibille, Ph.D, CAMH, 250 College Street, room 134, Toronto, ON M5T 1R8, Canada
E-mail: Etienne.sibille@camh.ca

Thomas D. Prevot, Ph.D., CAMH, 250 College Street, room 131, Toronto, ON M5T 1R8, Canada
Tel: 416-535-8501, ext 33785; E-mail: thomas.prevot@camh.ca

ABSTRACT

Background: Dysregulated tau phosphorylation is one of the hallmarks of Alzheimer's disease (AD), and it results in cognitive impairments, neuronal atrophy, and neurofibrillary tangle accumulation. Evidence shows that impaired somatostatin (SST) expression, particularly in SST-expressing GABAergic neurons, significantly contributes to AD-related pathophysiology and may increase cognitive burden. Additionally, SST+ interneurons in cortical layers and the hippocampus inhibit the dendrites of excitatory neurons, primarily through α5-GABAA receptors involved in cognitive regulation. Leveraging the potential of a newly developed small molecule that targets the α5-GABAA receptors via positive allosteric modulation (α5-PAM), we aim to assess its effects on tau phosphorylation-related neuronal morphology, cognitive deficits and protein expression.

Methods: In the PS19 transgenic mouse mode, we administered the α5-PAM, GL-II-73, either acutely or chronically at 3 and 6 months. We assessed spatial working memory using the Y-maze. Golgi staining analyzed dendritic morphology in chronically exposed mice to α5-PAM. Western blotting was used to quantify p-Tau and Tau expression.

Results: α5-PAM effectively reverses spatial working memory deficits induced by tau phosphorylation both acutely and chronically. Chronic treatment at 3and 6 months mitigates tau-induced loss of spine density. However, α5-PAM does not directly influence p-Tau levels, suggesting cognitive and neurotrophic benefits of GL-II-73s are independent of Tau burden.

Conclusions: These results demonstrate the potential for both symptomatic and disease-modifying effects, highlighting the promise of α5-GABAA receptor positive allosteric modulation as a novel therapeutic strategy for addressing cognitive deficits associated with tau phosphorylation in AD pathology.

INTRODUCTION

Alzheimer's disease (AD) is characterized by a spectrum of cognitive impairments, including altered executive functions, compromised working memory, impaired spatial memory and others. Among the complex biological changes associated with AD, the accumulation of Tau proteins or neurofibrillary tangles (NFTs) stands out as a prominent hallmark in the neurodegenerative process (*1*) in addition to amyloid β deposition. NFTs are made of hyperphosphorylated aggregates of the microtubule associated protein Tau (p-Tau) (*2*). Accumulation of phosphorylated Tau in AD has been linked to neuronal atrophy and cognitive deficits progression (*3*).

Despite clear understanding of the role of p-Tau aggregates in NFTs and amyloid plaques in the pathophysiology of AD, pharmacotherapies targeting amyloid β and tau have had limited success until the recent approval of antibody-based therapies targeting the insoluble amyloid protein (*4*). Therapies targeting the tau-pathology are being explored, such as Zagotenemab (a humanized anti-tau antibody(*5*)), LMTX (TauRx, an aggregation inhibitor (*6*)) TPI-287 (a microtubule stabilizer, (*7*)) and others, but so far none have demonstrated efficacy.

While the amyloid β and p-Tau are known to be major contributors to AD pathophysiology, it is well accepted that AD is a complex a multifactorial disease that may require a polypharmacopeia approach to reduce the burden of the disease on patient's quality of life (*8*). Consistently reported in the brain of AD patients is the hyperexcitability of the hippocampus (*9*) (brain region highly involved in cognitive functions (*10*)), that is proposed to be associated with tau-accumulation (*11*). This hyperexcitability is thought to be due in part to a loss of GABAergic inhibition (*12*). Evidence supports the contribution of GABAergic inhibition in the memory functions (*13*, *14*) and demonstrated that altered GABAergic signaling is linked to poorer cognitive functions in elderly (*15*) and in AD (*16*). Therefore, targeting the GABAergic system appears as a valid approach for reducing biological changes in AD pathology, and maybe provide symptom relief and disease-modifying effects.

A potential key player within the GABAergic system is somatostatin-expressing interneurons (SST+). SST+ interneurons mediate up to 60% of all GABAergic synaptic functions by exerting dendritic inhibition, a crucial process for balancing excitatory synaptic inputs. Most importantly,

SST+ interneurons loss has been reported in AD (*17*), comforting the idea that targeting the GABAergic system and more specifically improving altered SST+ interneuron signaling holds value in the treatment of AD.

SST+ interneurons signal in large part through the α5-GABAA receptors (α5-GABAA-R), which are of particular interest because of their discrete distribution in the hippocampus and prefrontal cortex (regions involved in cognitive processing). The α5-GABAA-R are localized synaptically and extrasynaptically in distal dendrites of pyramidal neurons. An especially promising treatment involves the exploration of compounds selectively modulating α5-GABAA-R (*18*). Previous studies in our group showed that targeting the α5-GABAA-R with the positive allosteric modulator GL-II-73 reverses cognitive deficits in animal models of stress (*19, 20*), aging (*21*), and amyloid deposition (*22*). In addition, we found that chronic treatment with GL-II-73 increased dendritic lengths, spine counts and spine density in the PFC and HIP of animals from the 3 models (*20-22*).

In the present study, we hypothesize that chronic α5-PAM treatment prevents or reverses neuronal deficits during the early stage of Tau tangle deposition and maybe at later stage which contributes to improved cognitive functions. To test this hypothesis, we investigated the potential of GL-II-73 to mitigate cognitive deficits and neuronal loss in the PS19 mouse model, characterized by the progressive accumulation of Tau tangles. The PS19 model expresses the P301S mutant form of human microtubule-associated protein tau (MAPT), under the direction of the mouse prion protein promoter (Prnp) (REF). These mice exhibit increased accumulation of Tau tangles, leading to cognitive decline and neuronal damage (*23*). We conducted assessments on both male and female mice at 3 and 6 months of age, representing early and late stages of Tau tangle deposition.

METHODS

Ethical Statement

All animal procedures adhered to the Ontario Animals for Research Act (RSO 1990, Chapter A.22) and the Canadian Council on Animal Care (CCAC). The study was approved by the Institutes Animal Care Committees (Protocol #846).

Animals

PS19 breeders, expressing the P301S mutant form of human microtubule-associated protein tau (MAPT), were obtained from Jackson Laboratories (Cat #008169-JAX) and paired with WT breeders to generate experimental groups' parents. Four cohorts of PS19 heterozygous (HET) and WT littermates were produced: Acute studies at 3 months (N=8 per group, 3 groups 54% male, **Fig. 1A**) and 6 months (N=8-9 per group, 3 groups, ~50% female, **Fig. 1B**); Chronic studies at 2-3 months (N=12-13 per group, 3 groups, 50% female, **Fig. 1C**) and 5-6 months (N=12-13 per group, 3 groups, 50% female, **Fig. 1D**). Animals were group-housed until the study commenced, then transitioned to single housing to facilitate drug administration and monitoring. They had ad libitum access to food and water and were maintained on a 12-hour light/dark cycle. Animal handling followed the techniques outlined in Marcotte et al (*24*) to minimize reactivity to the experimenter.

Drug Preparation and Administration

GL-II-73, an α5-GABAA receptor (α5-GABAA-R) positive allosteric modulator (PAM) (*19*), was synthesized by Dr. Cook's group (University of Wisconsin-Milwaukee). For acute administration via intraperitoneal (IP) injection, GL-II-73 was dissolved in a vehicle solution (85% distilled H2O, 14% propylene glycol (Sigma Aldrich), 1% Tween 80 (Sigma Aldrich)). Acute studies at 3 months and 6 months utilized GL-II-73 at 5mg/kg and 10mg/kg in the Y maze via IP injection, administered 30 minutes before testing. For chronic studies, GL-II-73 was dissolved in tap water and orally administered to mice at 30mg/kg, based on daily water intake calculations as in (*25*).

Y-Maze

The Y maze, adapted from Faucher et al. (*26*), uses spontaneous alternation to assess spatial working memory. It consists of three arms—two "goal" arms and one "starting" arm—separated by 120°, with sliding doors for the goal arms and a start box at the end of the starting arm. Mice undergo a 2-day habituation phase, exploring the maze for 10 minutes each day. On the third day, the training phase begins. Mice are placed in the start box, and after a 30-second interval, the sliding door opens, allowing them to choose a goal arm. After selection, the goal arm's door

closes, and the mouse stays there for 30 seconds before being returned to the start box. This is repeated for seven trials. On the fourth day, the procedure is repeated with a 60-second interval between trials, except for the eighth trial, where a 10-second interval tests motivation to alternate. Mice that do not alternate in the eighth trial are excluded to prevent motivational bias. Mean % alternation is calculated as [(Number of alternations/number of trials) * 100]. The maze is cleaned with 70% ethanol between trials to remove olfactory cues.

Golgi Staining and Analysis

After euthanasia and brain extraction, brains from six mice per group (three males, three females) were placed in Golgi Solution for two weeks, selected pseudo-randomly based on Y maze performance. They were then coded for blinded analysis and sent to NeuroDigitech (San Diego, CA, USA). Remaining brains were dissected for PFC and hippocampus extraction for western blot analysis.

For Golgi-stained brains, 100µm coronal slices were made using a cryostat and mounted on glass slides. Basal and apical dendrites of pyramidal neurons in layers II/III of the PFC and CA1 were identified as regions of interest (ROIs). Dendritic features were quantified using NeuroLucida v10 on a Zeiss Axioplan 2 microscope with an Optronics MicroFire CCD camera. Motorized X, Y, and Z focus enabled high-resolution imaging. Low magnification identified ROIs, while higher magnifications (40x-60x) were used for detailed analysis. Immersion oil and a Zeiss 100x lens facilitated 3D imaging and spine counting. Neurons (n=6 per animal) were selected based on complete dendritic filling and clear 3D visualization. Neurons with incomplete staining or visualization were excluded, and spine sampling focused on well-characterized spines orthogonal to the dendritic shaft. Data were analyzed using NeuroExplorer following (*27*).

Protein measurement via Western Blot

Brain tissue from the chronic 3- and 6-month groups (each consisting of 10 mice, with approximately 50% female) was prepared for protein analysis. The prefrontal cortex (PFC) and whole hippocampus regions were sonicated in APL buffer. Proteins were extracted from the brain homogenate using the AllPrep Kit (Qiagen, Germany). Protein concentrations were determined using the Bicinchoninic Acid (BCA) assay (Thermo Fisher Scientific, USA). Bovine

serum albumin (BSA) standards were used to generate a standard curve, and absorbance was measured at 562 nm with a microplate reader.

Equal amounts of protein (20 μg) from each sample, as determined by the BCA assay, were separated on 10% SDS-PAGE stain-free gels (Bio-Rad Laboratories, #5678094). Following electrophoresis, the gels were imaged using the ChemiDoc system (Bio-Rad Laboratories, USA) to verify equal loading and quantify total protein quantification. Proteins were then transferred onto nitrocellulose membranes using a semi-dry transfer system. Membranes were blocked with 5% BSA in 1X TBST (Tris-buffered saline with 0.1% Tween 20) for 1 hour at room temperature. Membranes were incubated overnight at 4°C with primary antibodies targeting PSD95, Gephyrin, Radixin, p-Tau or Tau (see **Supplementary Table 1** for details). After washing, membranes were incubated with HRP-conjugated secondary antibodies (Vector, #PI-1000 for rabbit and #PI-2000 for mouse) for 1 hour at room temperature. Signal detection was performed using an enhanced chemiluminescence (ECL) substrate (Thermo Fisher Scientific, USA) and the membrane was imaged in the ChemiDoc. Quantitative analysis of total protein and band intensity was conducted using ImageLab software.

Study Design

Heterozygote PS19 mice and their WT littermate were studied at 3 months of age (corresponding to an early stage of phosphorylation of tau; **Fig.1AB**) or at 6 months of age (corresponding to a more advanced stage of phosphorylation of tau; **Fig.1CD**). At each age, the effect of acute or chronic administration of GL-II-73 was investigated on working memory performances in the Y maze. In the chronic studies, brains were extracted for downstream analyses including morphology investigation using a Golgi staining technique, or western blot, 7 days after completion of the Y maze.

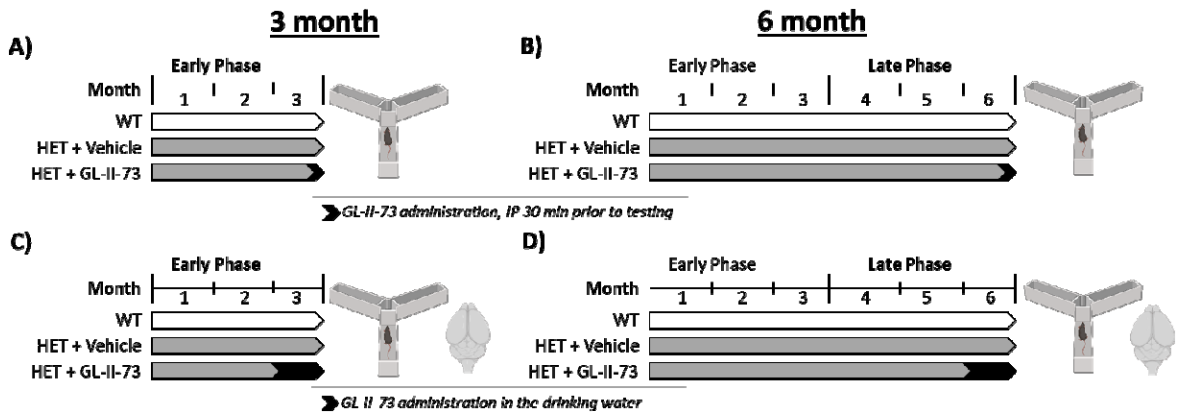

Figure 1. Study Design

Statistics

GraphPad Prism was employed for statistical analyses, and the results were graphically presented to convey mean ± SEM (**Supplementary Tables 2-4**). Morphological Golgi stain results were analyzed by Neurodigitech through two-way ANOVAs with Tukey's multiple comparisons test. The Y-maze data underwent analysis via Kruskal-Wallis test, followed by uncorrected Dunnett's multiple comparisons test. The pTau/Tsau ratio was calculated from the western blot relative expression of pTau and Tau, with the limitation that pTau levels in WT were not detectable. Therefore, relative expression was calculated using the HET group as a reference.

RESULTS

Chronic GL-II-73 treatment reverses neuronal shrinkage and reduces spine density in the PFC and CA1 of PS19 mice at 3 and 6 months.

Morphological changes on pyramidal neurons located in the prefrontal cortex (PFC) and the CA1 of the hippocampus (HIP) were quantified using a Golgi-Cox staining technique on mice from the chronic studies at 3 and 6 months.

In the PFC, untreated HET mice showed a significant reduction in spine density at 3 months and 6 months of age (**Figure 2**), which was significantly reversed by chronic administration of GL-II-73 at both ages (**Supplementary Table 2-3**). The spine density of HET treated with GL-II-73 (HET+GL) were significantly higher than untreated HET mice, and significantly lower than WT

mice. Similar reduction of spine density in untreated HET mice was observed in the CA1, while chronic GL-II-73 partially reversed it (**Figure 2; Supplementary Table 2-3**).

The reduction in spine density in HET mice and partial reversal with GL-II-73 treatment was observed at the apical and basal segment of the pyramidal (**Supplementary Figure 1**) in both the PFC and CA1. Changes in dendritic length and spine counts were also significant, marked by a reduction of length and spine count in untreated HET mice, and a reversal (partial or complete) with chronic GL-II-73 at both ages (**Supplementary Figure 2**).

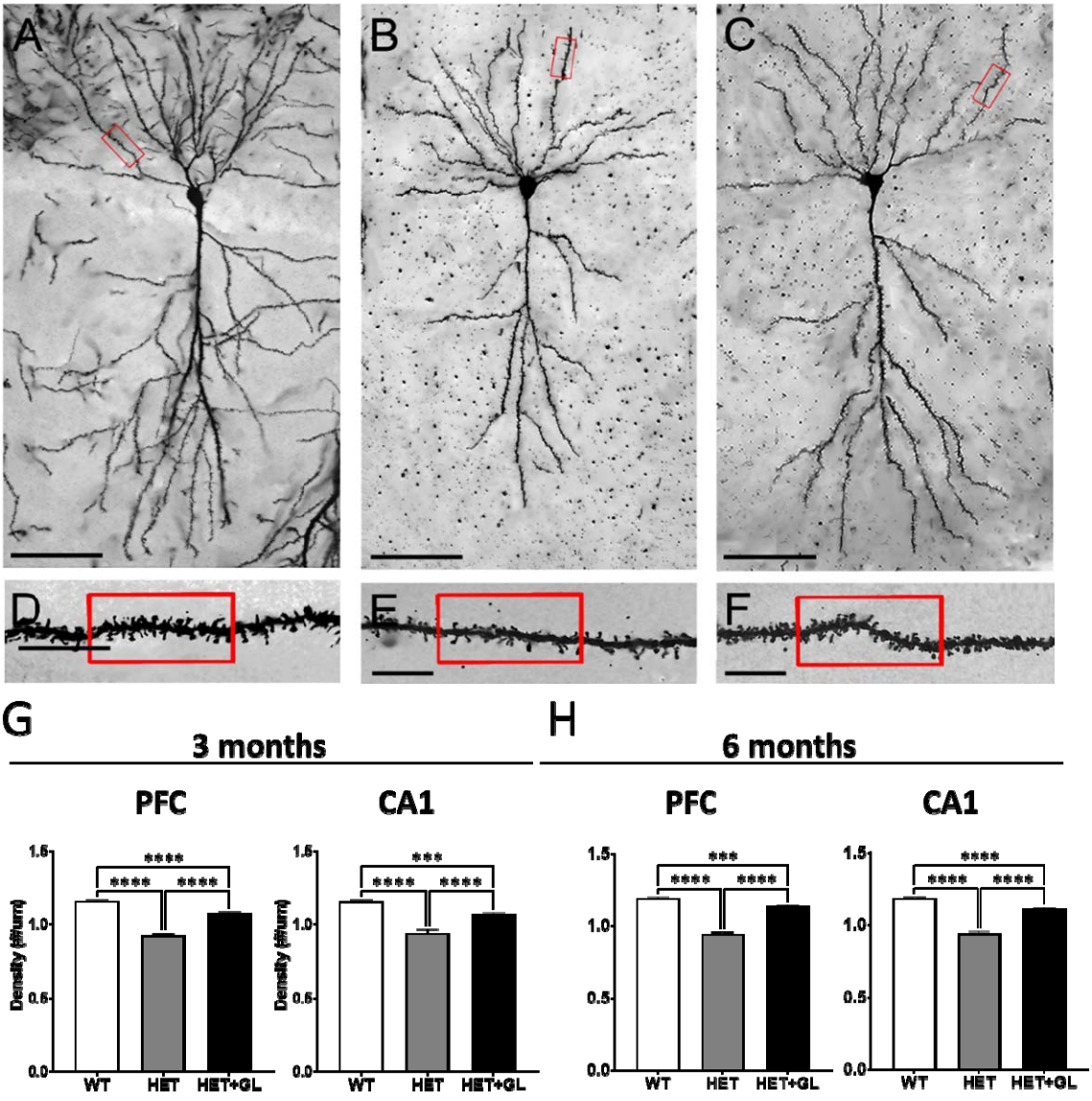

Figure 2. Chronic treatment with GL-II-73 increases spine density in the PFC and CA1 of PS19 mice at 3 and 6 months of age.

Chronic GL-II-73 does not affect the accumulation of phosphorylated Tau.

The prefrontal cortex and hippocampus from 9-10 animals that were not used for Golgi staining were collected to measure the accumulation of Tau and phospho-Tau after chronic administration of GL-II-73 at 3 and 6 months of age (**Supplementary Figure 3, and Supplementary Table 4**). There was no group differences in expression of tau in the PFC or HIP at 3 and 6 months. However, there was a significant increase in pTau levels in HET mice, and in HET+GL mice compared to WT. Taking the native expression of Tau and the expression of pTau in the same samples, a ratio between pTau/Tau was calculated as an index of disease progression (**Figure 3**). Heterozygote PS19 mice exhibited a significant increase in pTau/Tau ratio (driven by increase in pTau level; Supplementary Figure 3) in the PFC and HIP at 3 months and at 6 months. Mice receiving chronic administration of GL-II-73 also exhibited higher ratio of pTau/Tau compared to WT, which were not significantly different from untreated heterozygote PS19 mice in both brain regions, at both ages.

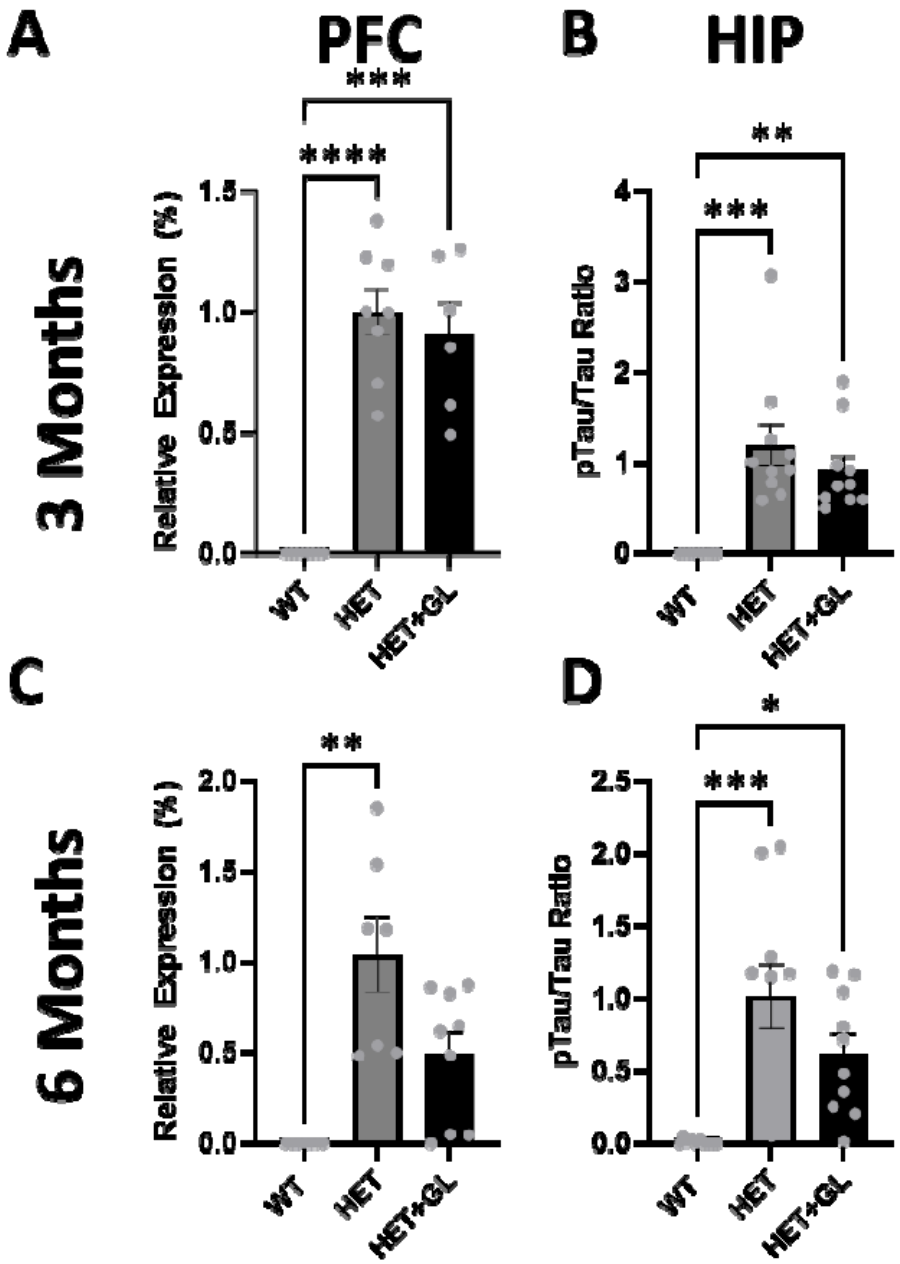

Figure 3. *pTau/Tau ratio in the PFC and HIP from PS19 mice treated with GL-II-73 compared to untreated PS19 and WT controls.*

Acute and chronic GL-II-73 treatment contributes to improvement in working memory.

Mice were trained in the alternation task in the Y maze, and tested at 3 months and 6 months, after either acute administration of GL-II-73, 30 minutes prior to testing, or after chronic administration in the drinking water for 4 weeks. In the groups of mice participating in the acute

studies (**Supplementary Figure 4, and Supplementary Table 5**), PS19 HET mice showed an alternation deficit compared to WT mice, at 3 and 6 months. Administration of GL-II-73 at 5 mg/kg did not significantly impact alternation rates, neither at 3 nor 6 months. Interestingly, administration of GL-II-73 at 10 mg/kg in 3 months-old HET mice significantly increased alternation rates to levels similar to WT. This effect was no longer significant at 6 months.

In the chronic administration studies (**Figure 4, and Supplementary Table 5**), alternation rates in the 3 months-old mice were not significantly different between group. Interestingly, at 6 months, the alternation rate deficit in PS19 HET mice compared to WT was observed, and reversed with chronic administration of GL-II-73.

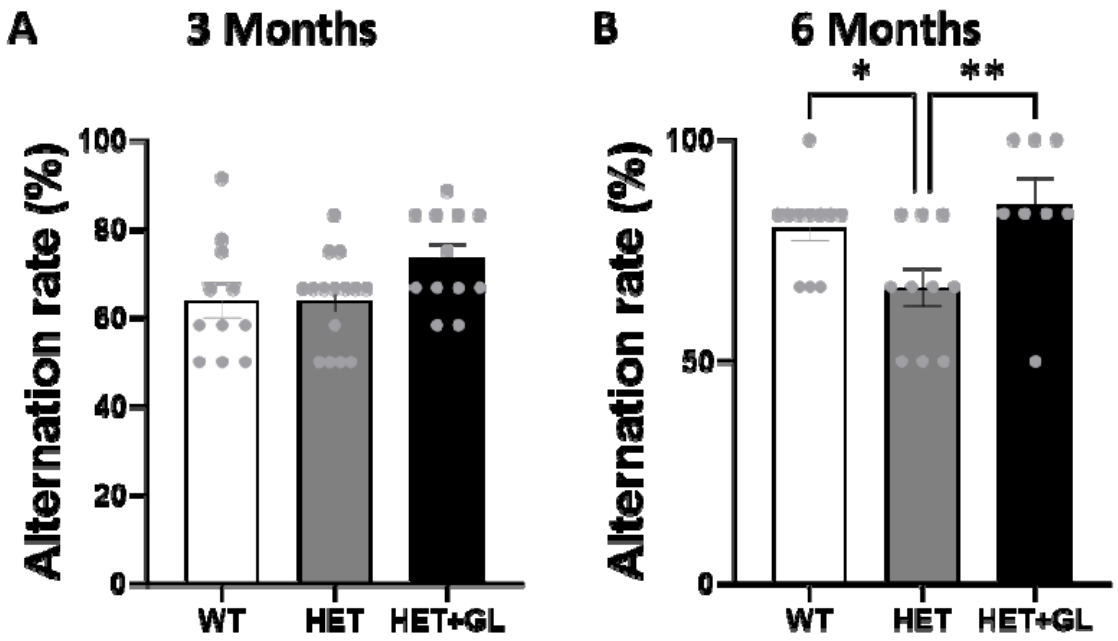

Figure 4. *Effects of chronic administration of GL-II-73 on alternation rate in PS19 HET mice*

DISCUSSION

This study demonstrated that chronic administration of GL-II-73, a positive allosteric modulator of the α5-GABAAR (*28*), increases spine density in the prefrontal cortex and hippocampus of the PS19 mice despite accumulation of tau tangles. In addition, improvement of cognitive functions, and more specifically working memory was observed, in particular at 3 months when given

acutely, and 6 months of age when given chronically. Importantly, the beneficial effects on neuronal morphology and cognitive functions was independent of tau-levels, since the chronic treatment did not reduce the tau tangle accumulation.

These findings aligned with previous findings in other models, demonstrating that targeting the α5-GABAA-Rs with GL-II-73 has neurotrophic effect in the PFC and CA1, as well as cognitive benefits. Indeed, our group demonstrated that chronic administration of GL-II-73 reverses working memory deficits and neuronal atrophy in animal models of chronic stress (*19, 20*), aging (*21*), and amyloid deposition (*22*).

Targeting GABAergic neurotransmission, particularly through α5-GABAA R, offers a promising avenue for AD research. These receptors are predominantly expressed in hippocampal regions, crucial for memory and cognition (*18*), areas severely affected in AD. Dysregulation of GABAergic signaling in AD has been linked to cognitive decline, and modulating α5 GABAA-R activity could help restore inhibitory balance and improve cognitive function (*18*). Moreover, combining this approach with anti-tau therapies could provide synergistic effects, as tau pathology contributes to neurodegeneration and cognitive impairment. By simultaneously addressing both tau accumulation, GABAergic dysfunction and neuronal loss, combination therapies have the potential to enhance treatment efficacy and slow disease progression.

FUNDING

This work has been funded by the Weston Brain Institute (TR192043).

ACKNOWLEDGEMENTS

Authors thank Mehrab Ali for support with administrative tasks throughout the study, the CAMH animal facility staff for the caring for our animals over the study duration, the members of NeuroDigitech for their contribution to data generation, and all the animals that contributed to these studies.

DISCLOSURES

JMC, MM, ES and TP are listed inventors on patents covering syntheses and use of the compound. ES is Founder and CSO of Damona Pharmaceuticals, a biopharma dedicated to bring

novel GABAergic compounds to the clinic. TP is the acting Director of Preclinical Research and Development in Damona. All other authors declare no conflicts of interest.

References

1. R. Medeiros *et al.*, The role of tau in Alzheimer's disease and related disorders. *CNS Neurosci Ther* **17**, 514-524 (2011).
2. S. Muralidar *et al.*, Role of tau protein in Alzheimer's disease: The prime pathological player. *International Journal of Biological Macromolecules* **163**, 1599-1617 (2020).
3. A. Bejanin *et al.*, Tau pathology and neurodegeneration contribute to cognitive impairment in Alzheimer's disease. *Brain* **140**, 3286-3300 (2017).
4. B. Dunn *et al.*, Approval of aducanumab for Alzheimer disease—the FDA's perspective. *JAMA internal medicine* **181**, 1276-1278 (2021).
5. B. A. Willis *et al.*, Safety, Tolerability, and Pharmacokinetics of Zagotenemab in Participants with Symptomatic Alzheimer's Disease: A Phase I Clinical Trial. *J Alzheimers Dis Rep* **7**, 1015-1024 (2023).
6. D. Seripa *et al.*, Tau-directed approaches for the treatment of Alzheimer's disease: focus on leuco-methylthioninium. *Expert Review of Neurotherapeutics* **16**, 259-277 (2016).
7. S. A. Goldlust *et al.*, Phase 1 trial of TPI 287, a microtubule stabilizing agent, in combination with bevacizumab in adults with recurrent glioblastoma. *Neuro-Oncology Advances* **6**, (2024).
8. K. Iqbal *et al.*, Alzheimer's disease, a multifactorial disorder seeking multitherapies. *Alzheimers Dement* **6**, 420-424 (2010).
9. S. E. Setti *et al.*, Alterations in hippocampal activity and Alzheimer's disease. *Translational issues in psychological science* **3**, 348 (2017).
10. E. T. Rolls *et al.*, The effective connectivity of the human hippocampal memory system. *Cerebral Cortex* **32**, 3706-3725 (2022).
11. W. Huijbers *et al.*, Tau Accumulation in Clinically Normal Older Adults Is Associated with Hippocampal Hyperactivity. *The Journal of Neuroscience* **39**, 548-556 (2019).
12. J. Jiménez-Balado *et al.*, GABAergic dysfunction, neural network hyperactivity and memory impairments in human aging and Alzheimer's disease. *Seminars in Cell & Developmental Biology* **116**, 146-159 (2021).
13. L. Topolnik *et al.*, The role of inhibitory circuits in hippocampal memory processing. *Nature Reviews Neuroscience* **23**, 476-492 (2022).
14. B. Bie *et al.*, Suppression of hippocampal GABAergic transmission impairs memory in rodent models of Alzheimer's disease. *European Journal of Pharmacology* **917**, 174771 (2022).
15. J. Jiménez-Balado *et al.*, Reduced Hippocampal GABA+ Is Associated With Poorer Episodic Memory in Healthy Older Women: A Pilot Study. *Frontiers in Behavioral Neuroscience* **15**, (2021).
16. Y. Li *et al.*, Reversible GABAergic dysfunction involved in hippocampal hyperactivity predicts early-stage Alzheimer disease in a mouse model. *Alzheimer's Research & Therapy* **13**, 114 (2021).
17. R. Waller *et al.*, Histological characterization of interneurons in Alzheimer's disease reveals a loss of somatostatin interneurons in the temporal cortex. *Neuropathology* **40**, 336-346 (2020).
18. T. Prevot *et al.*, Altered GABA-mediated information processing and cognitive dysfunctions in depression and other brain disorders. *Mol Psychiatry* **26**, 151-167 (2021).
19. T. D. Prevot *et al.*, Novel Benzodiazepine-Like Ligands with Various Anxiolytic, Antidepressant, or Pro-Cognitive Profiles. *Mol Neuropsychiatry* **5**, 84-97 (2019).

20. A. Bernardo *et al.*, Symptomatic and neurotrophic effects of GABAA receptor positive allosteric modulation in a mouse model of chronic stress. *Neuropsychopharmacology* **47**, 1608-1619 (2022).
21. T. D. Prevot *et al.*, Reversal of Age-Related Neuronal Atrophy by alpha5-GABAA Receptor Positive Allosteric Modulation. *Cereb Cortex* **31**, 1395-1408 (2021).
22. A. M. Bernardo *et al.*, Positive allosteric modulation of α5-GABA A Receptor in the 5XFAD mouse model has cognitive and neurotrophic benefits. *bioRxiv*, 2022.2009.2030.510361 (2022).
23. S. Zampar *et al.*, Characterization of a Mouse Model of Alzheimer's Disease Expressing Aβ4-42 and Human Mutant Tau. *International Journal of Molecular Sciences* **22**, 5191 (2021).
24. M. Marcotte *et al.*, Handling Techniques to Reduce Stress in Mice. *J Vis Exp*, (2021).
25. T. D. Prevot *et al.*, Reversal of Age-Related Neuronal Atrophy by α5-GABAA Receptor Positive Allosteric Modulation. *Cereb Cortex* **31**, 1395-1408 (2021).
26. P. Faucher *et al.*, Hippocampal Injections of Oligomeric Amyloid β-peptide (1-42) Induce Selective Working Memory Deficits and Long-lasting Alterations of ERK Signaling Pathway. *Front Aging Neurosci* **7**, 245 (2015).
27. C. C. Wu *et al.*, Selective vulnerability of dentate granule cells prior to amyloid deposition in PDAPP mice: digital morphometric analyses. *Proc Natl Acad Sci U S A* **101**, 7141-7146 (2004).
28. T. D. Prevot *et al.*, Residual avoidance: A new, consistent and repeatable readout of chronic stress-induced conflict anxiety reversible by antidepressant treatment. *Neuropharmacology* **153**, 98-110 (2019).

FIGURE CAPTIONS

Figure 1. Study Design

Heterozygote PS19 mice (HET) and their wildtype (WT) littermates were included in these studies, assessing the effect of GL-II-73 on working memory and neuronal morphology. Acute treatment (**A-B**) was provided to the animals via intraperitoneal administration at 5mg/kg or 10mg/kg at 3 (**A**) or 6 (**B**) months of age. Chronic administration of GL-II-73 was also investigated at 3 (**C**) and 6 (**D**) months, with 4 weeks of administration in the drinking water at 30 mg/kg. One week after completion of the behavioral screen, mice were euthanized by rapid cervical dislocation. Brains from 4 mice per group were collected for Golgi staining, while the remaining 8 per group were collected for WesternBlot analyses.

Figure 2. Chronic treatment with GL-II-73 increases spine density in the PFC and CA1 of PS19 mice at 3 and 6 months of age.

Four brains per group were collected after chronic administration of GL-II-73 at 3 and 6 months. Six pyramidal neurons in the PFC (illustrated in A-F) and 6 principal cells of the CA1 of the HIP were isolated per animal and quantified for dendritic length and spine counts. Spine density was established in both regions (PFC (**G**) and CA1 (**H**)). Untreated HET mice showed a significant reduction in spine density at 3 months in the PFC and CA1 which were partially reversed by chronic GL-II-73 (**G**). Similar effects were observed at 6 months (**H**). ***$p<0.001$, ****$p<0.0001$. Mean ±SEM.

Figure 3. pTau/Tau ratio in the PFC and HIP from PS19 mice treated with GL-II-73 compared to untreated PS19 and WT controls.

Using Western Blot targeting Tau and p-Tau, a p-Tau/Tau ration was calculated. HET mice at 3 months of age showed a higher ratio compared to WT (as expected) in the PFC (**A**) and HIP (**B**). HET mice receiving chronic GL-II-73 administration also showed higher ratio compared to WT, not different from untreated HET mice. At 6 months, the increased ratio in untreated HET compared to WT was confirmed in the PFC (**C**) and HIP (**D**). HET mice receiving GL-II-73 showed ratio not different from WT or HET in the PFC, and significantly higher than WT in the HIP. **$p<0.01$, ***$p<0.001$, ****$p<0.0001$. Mean ±SEM.

Figure 4. Effects of chronic administration of GL-II-73 on alternation rate in PS19 HET mice

Alternation rate in the Y maze were measured after chronic administration of GL-II-73 at 3 motnhs (**A**) and 6 months (**B**). At 3 months, there was no difference between groups. At 6 months, untreated HET mice showed a significantly reduced alternation rate compared to WT. On the other hand, HET mice receiving GL-II-73 showed significantly higher alternation rate than untreated HET. *$p<0.05$, **$p<0.01$. Mean ±SEM.

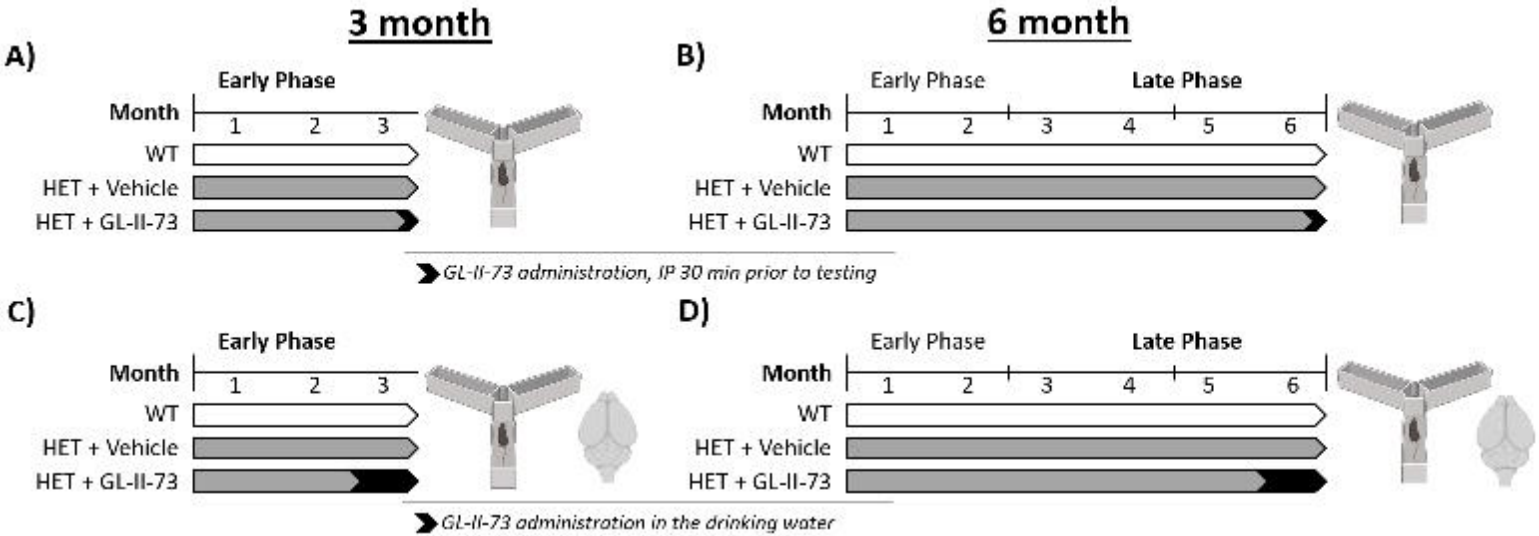
3 month
6 month
A)
B)
C)
D)
Early Phase
Late Phase
Month
1
2
3
4
5
6
WT
HET + Vehicle
HET + GL-II-73
GL-II-73 administration, IP 30 min prior to testing
GL-II-73 administration in the drinking water

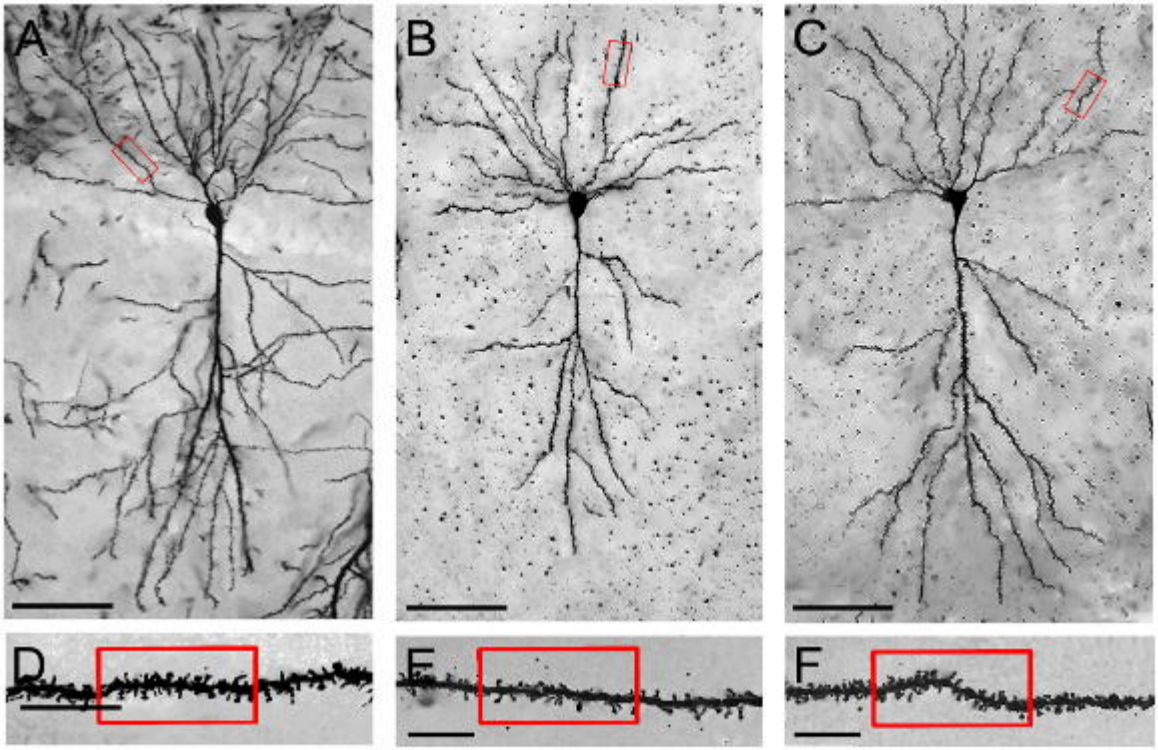
A
B
C
D
E
F

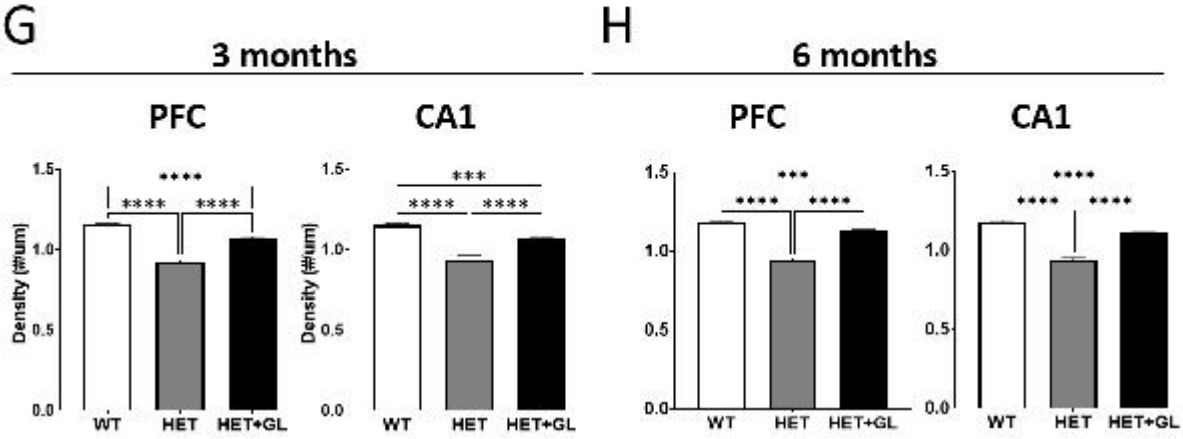
G
3 months
PFC
CA1
H
6 months
PFC
CA1
Density (#/um)
1.5
1.0
0.5
0.0
****
***
WT
HET
HET+GL

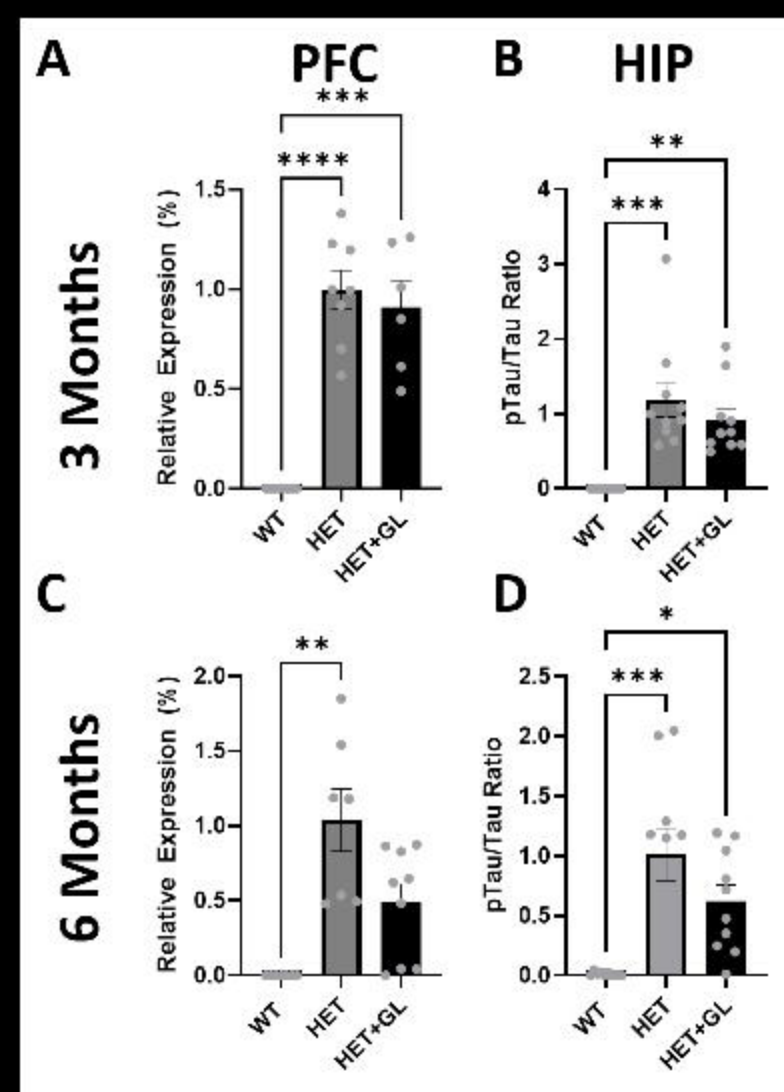
A
PFC
B
HIP
3 Months
Relative Expression (%)
pTau/Tau Ratio
WT
HET
HET+GL
C
D
6 Months

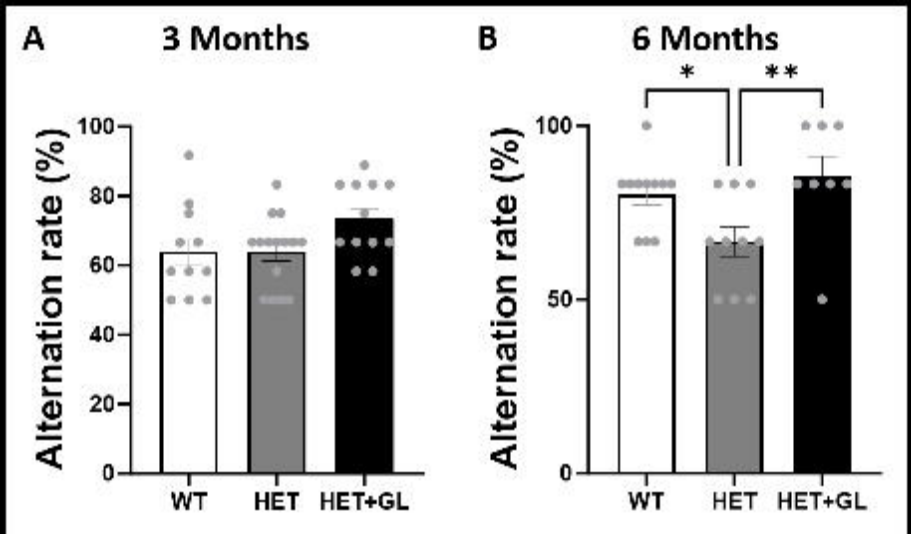
A
3 Months
Alternation rate (%)
100
80
60
40
20
0
WT
HET
HET+GL
B
6 Months
*
**
Alternation rate (%)
100
50
0
WT
HET
HET+GL